American Mineralogist, Volume 62, pages 528–533, 1977

Mechanisms of transformation and twinning in gillespite at high pressure

ROBERT M. HAZEN[1]

Department of Mineralogy and Petrology, University of Cambridge
Cambridge, England CB2 3EW

Abstract

Single-crystal X-ray data on gillespite ($BaFeSi_4O_{10}$) indicate a unit-cell volume discontinuity at the high-pressure red-to-blue (gillespite I-to-gillespite II) transition. Thus the tetragonal-to-orthorhombic phase transformation is of first order. Two forms of twinning were observed in the high-pressure phase, with the twin laws: 4-fold axis parallel to *c*, and 2-fold axis parallel to [110]. Both twin laws are symmetry elements of the tetragonal low-pressure phase, in which no twinning was observed.

The geometries of the gillespite I and II silicate layers are examined and transformation and twinning mechanisms are proposed.

Introduction

Gillespite ($BaFeSi_4O_{10}$) has attracted considerable attention in recent years, despite its relative rarity in nature. This interest may be ascribed to the unusual square-planar coordination of iron, and a striking red-to-blue reversible phase transformation at ≈12 kbar.[2] Hazen and Burnham (1974, 1975) described the crystal structures of gillespite I (at 1 atm) and gillespite II (at ≈12kbar), and noted changes in both symmetry and unit-cell dimensions of the two phases. Specifically, gillespite I at room pressure is tetragonal, $P4/ncc$, a = 7.516, c = 16.077 A, Z = 4; the structure possesses a pseudo-repeat of 8 A parallel to c, but alternate silicate layers have clockwise and anti-clockwise rotations respectively. Gillespite II is orthorhombic, $P2_12_12$, a = 7.349, b = 7.516, c = 7.894 A, Z = 2; all layers have the same rotational direction. Hazen and Burnham (1974) suggested that observed shifts in the silicate layers allowed significant collapse of the 8-coordinated barium site, and thus a reduction of molar volume in the gillespite I → II transition. Recently, Huggins *et al.* (1976) have observed a second transition to gillespite III at a pressure of approximately 70 kbar.

Hazen and Burnham did not examine gillespite at intermediate pressures, and there was thus no conclusive evidence that the color change, symmetry changes, and unit-cell changes were simultaneous and related. Furthermore, since gillespite I and II are topologically identical and the transition is rapid and reversible, it was not proved whether the change was of first or second order. The principal objectives of this investigation are:

(1) to observe continuous and discontinuous changes in gillespite unit-cell parameters and optical properties to pressures exceeding the red-to-blue transition;

(2) to determine whether the transformation is of first or second order;

(3) to examine the orthorhombic high-pressure phase for possible twinning induced by the reduction of symmetry from tetragonal;

(4) to suggest transformation and twinning mechanisms for gillespite based on geometrical constraints of the two structures.

Experimental

A single crystal of gillespite from Fresno County, California, was selected from the same material described by Hazen and Burnham (1974). The 150 × 130 × 40 μm cleavage plate was mounted in index-of-refraction oil in a miniature pressure cell (Merrill and Bassett, 1974) with (001) cleavage planes parallel to the flat diamond faces. Precession and cone-axis photographs were taken at eight increments of pressure to well above the 12 kbar transition. The red-to-blue

[1] Present address: Geophysical Laboratory, 2801 Upton St., N. W., Washington, D. C. 20008.

[2] Strens (1966) recorded a transformation pressure of 26 kbar for gillespite I→II. However, recent work by Huggins *et al.* (1976) indicates the transition pressure is 12 ± 1 kbar.

transformation was observed between the fifth and sixth increment, and while no internal pressure calibration was available, the pressure at the eighth (highest pressure) increment was undoubtedly in excess of 15 kbar.

Twinning at high pressure

No twinning was observed in gillespite II following the first set of pressure increments. However, the pressure was released and reapplied several times, cycling across the I–II transition. Each time the pressure was changed, the crystal was examined both optically and with X-rays. The tetragonal low-pressure phase was always optically homogeneous, and gave a sharp single-crystal *c*-axis 0-level precession photograph. However, the orthorhombic gillespite II displayed more varied behavior. Following several of the gillespite I to II transitions, one of two distinct forms of twinning was observed.

A 90° rotation parallel to [001] was the most frequently encountered high-pressure twin operator, and was found in more than half of the cycles. Crys-

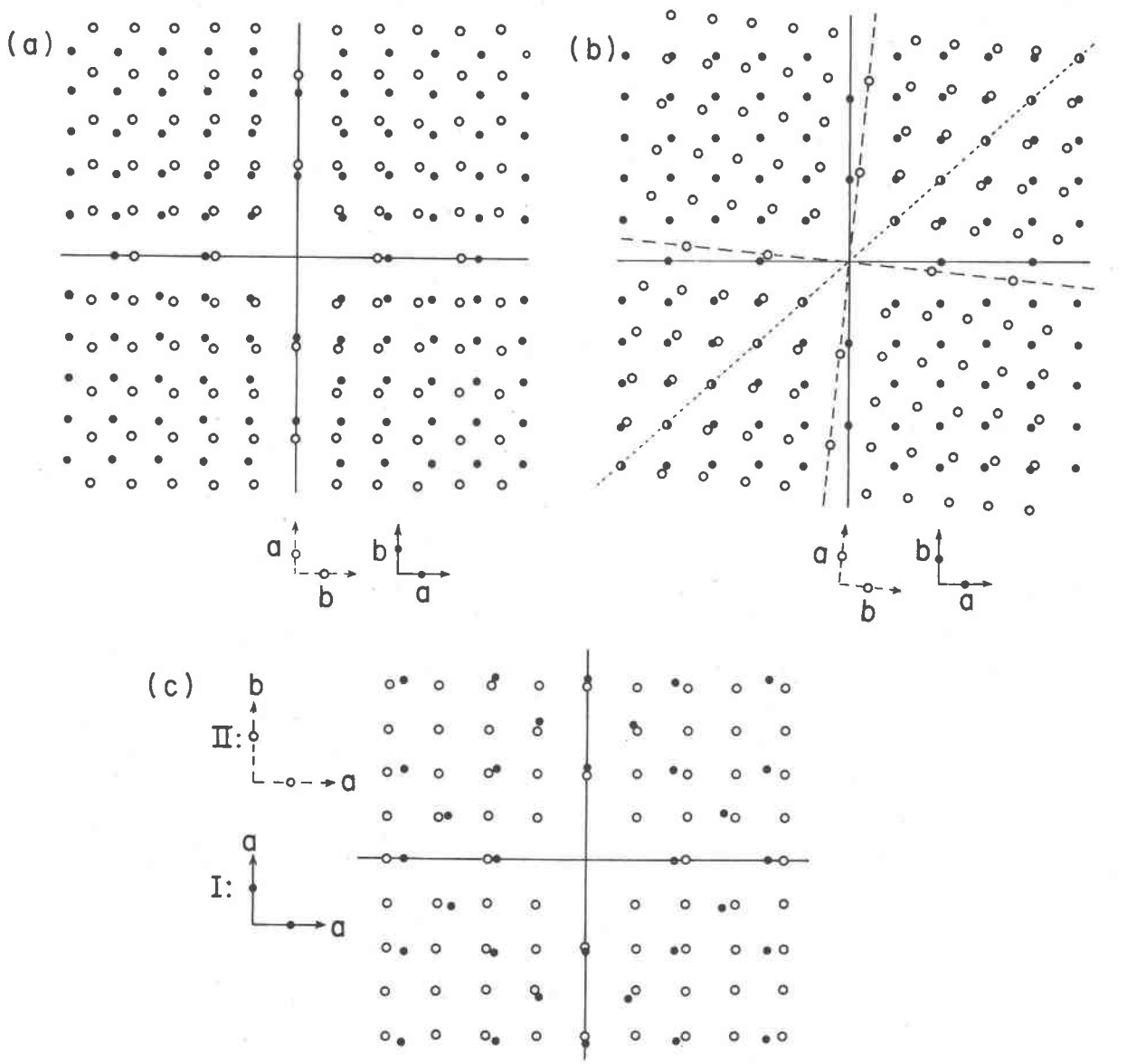

Fig. 1. Reciprocal lattice geometries of gillespite II twins, and coexisting gillespite I and II. The (*hk*0) nets are illustrated for (a) four-fold axis parallel to [001] twin operation; (b) two-fold axis parallel to [110] twin operation; and (c) coexisting gillespite I and II. The difference between *a* and *b* in orthorhombic gillespite II has been exaggerated for clarity.

tals twinned in this way are optically homogeneous in (001). The composition plane is thought to be (001) due to this optical evidence, and to geometrical considerations (see discussion below). Diffraction geometry produced by the 90° rotation twin is illustrated in Figure 1a; the ratio of volumes of the two twin components (as estimated from relative intensities of equivalent reflections) varied considerably from cycle to cycle.

The second twin operator, observed in two of the cycles, is a 180° rotation parallel to [110] of the tetragonal phase. This twin is distinguished by its diffraction geometry (Fig. 1b) and by twin regions visible in the (001) cleavage plate. The composition surface is irregular, but appeared to be approximately at right angles to (001) in the two cases examined.

It should be noted that the twin laws could be described in other ways; the twin operators selected are also symmetry operators of the tetragonal gillespite I phase.

Coexisting gillespite I and II

During the first ten cycles the crystal occupied a small fraction of the pressure-gasket volume, and phase transitions were rapid and complete. However, repeated tightening and loosening of the pressure cell tends to cause slight loss of pressure fluid, and the steel gasket may thus crush and distort. In this way the possibility of non-hydrostatic pressure effects may be introduced. On the twelfth cycle the crystal did not transform uniformly—the center of the gillespite plate turned blue before the edges. Small changes in the tightening of the pressure screws allowed continuous movement of the red–blue interface. Since only a slight turn of the pressure screws was required to transform from all-red to all-blue, it is assumed that the pressure gradient was less than 1 kbar. It was possible to hold the crystal with both gillespite I and II coexisting, and the small continuous pressure gradient across the crystal allowed the evaluation of several important properties of the red-to-blue transition. These properties include the unit-cell dimensions of the coexisting polymorphs, the relative orientations of the coexisting lattices, and the orientation of the gillespite I–II interface.

Discontinuous changes observed at the gillespite I–II transition include:

(1) a color change from red to blue;

(2) an increase in the optical relief from low to high (*i.e.* an increase in refractive index);

(3) a halving of the *c* axis;

(4) a change of tetragonal *a* axis from 7.47 A to orthorhombic $a = 7.349$ and $b = 7.515$ A;

(5) a change in unit sub-cell volume from 444 A^3 to 436 A^3;

(6) a reduction of symmetry from $P4/ncc$ to $P2_12_12$.

Figure 1c illustrates the reciprocal lattice geometry of coexisting gillespite I and II, and is proof of the first-order changes in the gillespite phase transformation. A semi-quantitative plot of unit-cell parameters and volume *vs.* pressure (based in part on data from Hazen and Burnham, 1974) is presented in Figure 2. In many oxides and silicates, compression is approximately linear with pressure to 30 kbar, and this assumption has been made in Figure 2.

Discussion

Geometry of the gillespite layer

The ideal gillespite structure is $P\,4/n\,2_1/m\,2/m$, $c = 8$A, and the symmetry of the ideal silicate layer is $4mm$ in *c*-axis projection (Fig. 3a).[3] Gillespite I repre-

[3] The ideal gillespite structure has not yet been observed. High-temperature experiments are now in progress to search for this possible form.

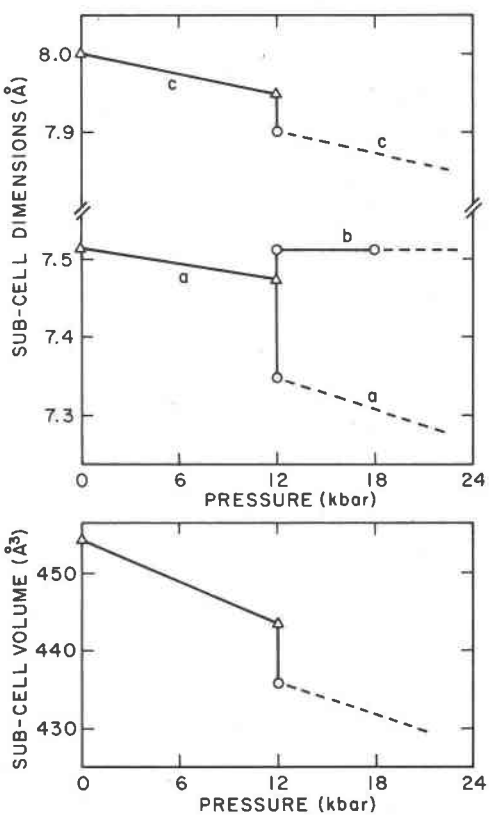

Fig. 2. Semi-quantitative plots of gillespite sub-cell dimensions and volume versus pressure. Known points are marked by Δ's (gillespite I) and ○'s (gillespite II). Data in part from Hazen and Burnham (1974).

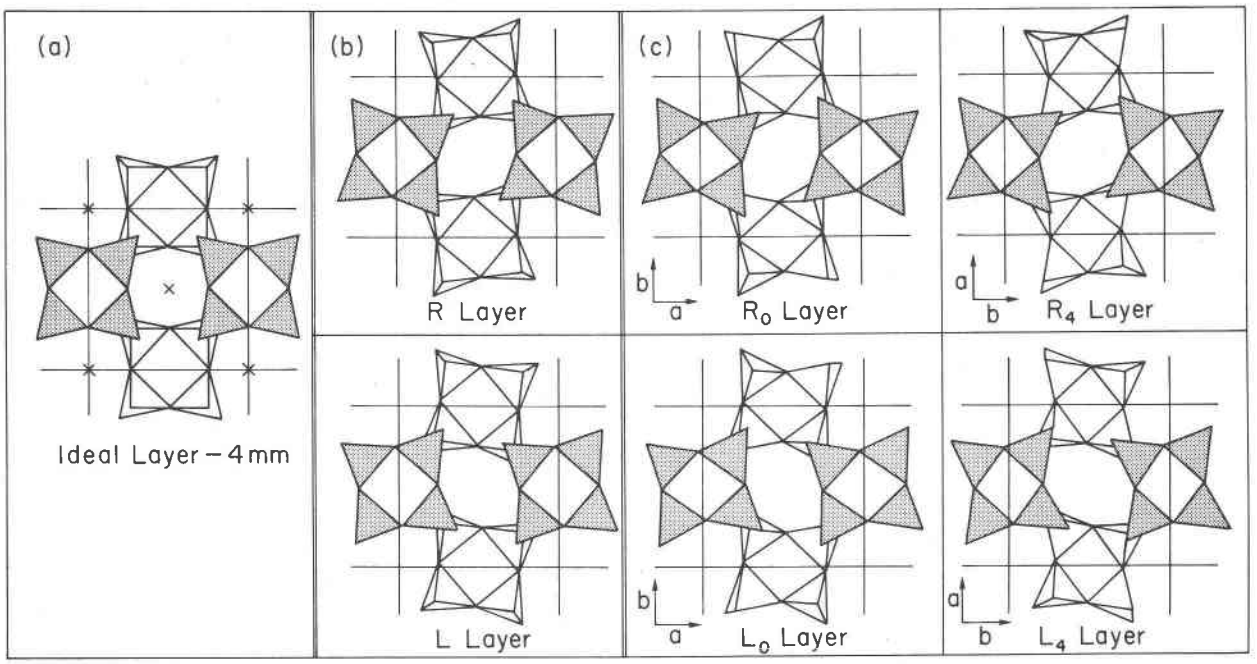

Fig. 3. The layer types of gillespite in *c*-axis projection. (a) The ideal gillespite layer, *4mm*. The *X*'s indicate positions of interlayer Ba cations. (b) Gillespite I layers, 4. The two possible orientations have been labelled *R* and *L* based on the relative rotation of the upper four-membered ring. (c) Gillespite II layers, 2. Four possible orientations have been labelled R_0, L_0, R_4, and L_4 based on relative rotation of the upper four-member ring, and orientation of the *a* and *b* axes.

sents a slight distortion of the ideal structure, and has reduced layer symmetry of 4. Due to the mirror-violating rotation of the four-tetrahedra rings, there are two possible orientations of the gillespite I layer. These are illustrated in Figure 3b and are labelled *R* and *L* for the relative right- and left-handed 5° rotations of the upper layer. These *R* and *L* layers are a non-superimposable enantiomorphic pair. In gillespite I, the observed layer-stacking arrangement is (*RLRLRL* . . .), giving a double-layer 16 A repeat. While stacking faults have not been detected, it seems probable, given the similar geometry of the two layers, that defects in stacking sequence could occur.

Gillespite II represents a further distortion of the ideal gillespite structure, and the layer symmetry is 2. Four distinct orientations of the pseudo-*4mm* silicate layer are shown in Figure 3c, and are called R_0, R_4, L_0, and L_4, depending on rotation direction of the top four-member ring (*R vs. L*) and the orientation of *a* and *b* axes with respect to the first layer (0 *vs.* 4). The ideal gillespite II is a simple repeat of one orientation (*i.e.* $R_0R_0R_0 \cdots \equiv R_4R_4R_4 \cdots$; or, $L_0L_0L_0 \cdots \equiv L_4L_4L_4 \cdots$, which is the enantiomorphous form). However, it is easy to visualize stacking faults and other variations in gillespite II; these variations are the origin of twinning in orthorhombic gillespite.

Mechanisms of transformation

The positions of iron and barium cations are virtually the same for both gillespite I and II, and for any layer orientation. It is therefore necessary to examine the silicate layers for the key to gillespite's transformation behavior. The transition of layers may be schematically represented as (*RLRLRL* $\cdots$) $\rightarrow$ ($R_0R_0R_0R_0 \cdots$), or taken layer-by-layer, ($R \rightarrow R_0$), ($L \rightarrow R_0$), ($R \rightarrow R_0$), *etc.* The shift from *R* to R_0 requires only a slight distortion of the layer from 4 to 2 layer symmetry. However, the change from *L* to R_0 involves both a distortion and a 10° rotation of the four-tetrahedra rings. This is the discontinuous struc-

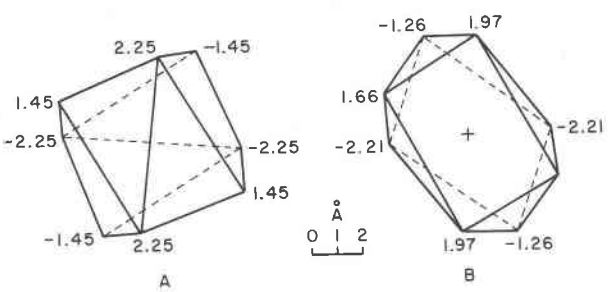

Fig. 4. Barium coordination polyhedra in *c*-axis projection: (a) gillespite I (b) gillespite II. Heights and scale are in A.

tural change responsible for the first-order gillespite I–II transition.

It is interesting to examine changes in barium's coordination polyhedron resulting from the change in layer geometry and stacking sequence. The barium cation is in an interlayer position, coordinated to four oxygen atoms of each of two adjacent silicate layers (see *X*'s in Fig. 3a). As illustrated in Figure 4, the gillespite I barium polyhedron has the topology of a cube, though it is quite distorted. Gillespite II, on the other hand, has a barium–oxygen coordination group with square antiprism topology. The latter polyhedron is smaller in mean Ba–O bond length and in volume, and is significantly shorter parallel to the *c* axis (3.55 *vs.* 3.70 A). Thus, the change in layer sequence from $(RLRLRL \cdots)$ to $(R_0R_0R_0R_0 \cdots)$ produces a considerable volume reduction in the high-pressure gillespite II.

Twinning geometries and mechanisms

Gillespite twinning geometries and mechanisms are best visualized using the layer diagrams of Figure 3c. The 4-fold axis parallel to [001] is the simplest twin operation to describe, and may be represented by

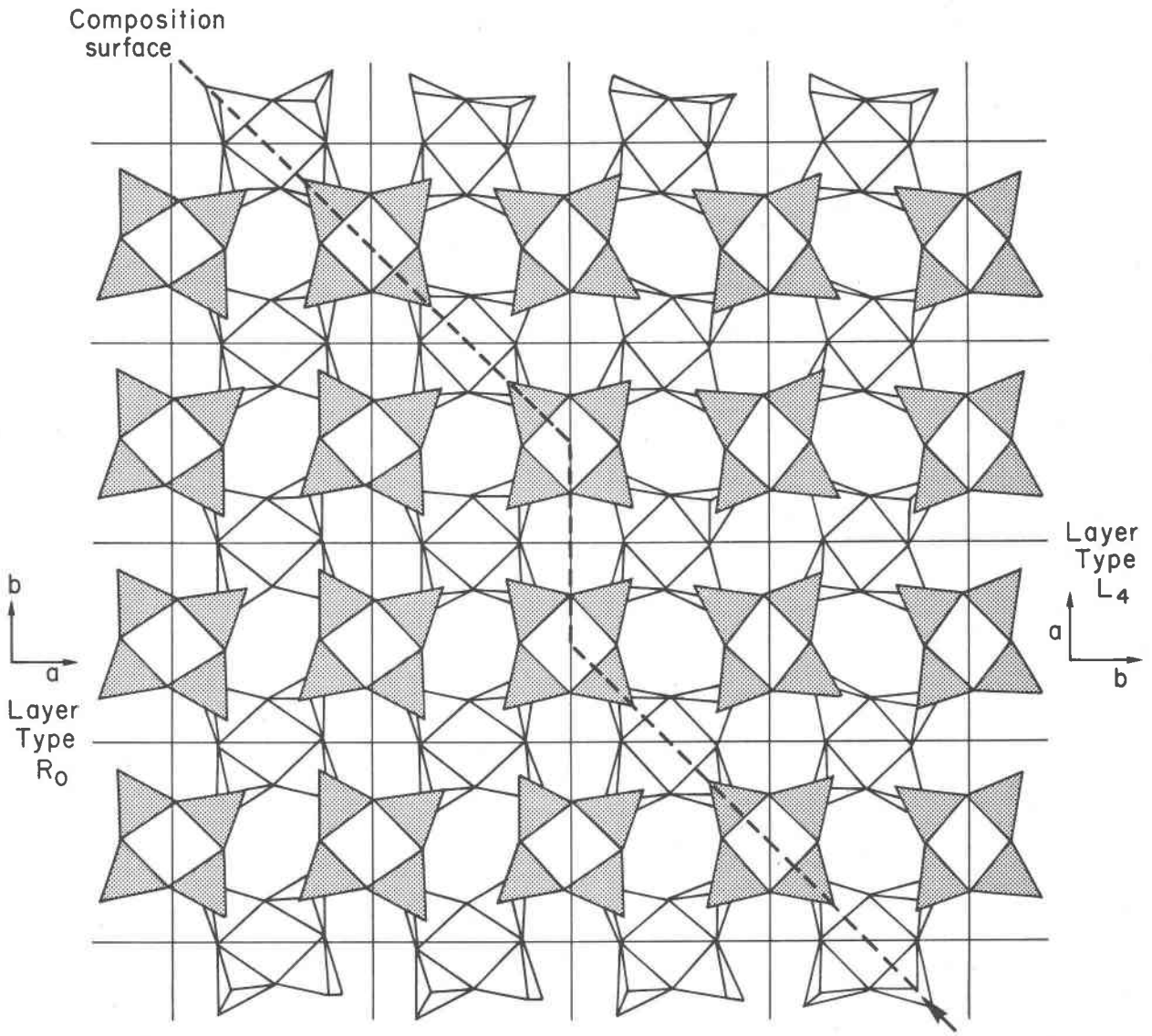

Fig. 5. Schematic diagram of the gillespite II [110] twin in *c*-axis projection. A 180° rotation parallel to [110] is the twin operator. The composition surface is irregular and passes through the (001) plane.

the layer sequence $(\cdots R_0R_0R_0|R_4R_4R_4\cdots)$ or $(\cdots R_0R_0R_0|L_4L_4L_4\cdots)$. Such a twin may arise when part of a gillespite I crystal transforms $(RLRL\cdots) \rightarrow (R_0R_0R_0\cdots)$ and part transforms $(RLRL\cdots) \rightarrow (R_4R_4R_4\cdots)$ or $(L_4L_4L_4\cdots)$. The composition plane will then be (001), which is consistent with the lack of optically-visible twin lamellae in the (001) section.

The two-fold axis parallel to [110] twin law is also the consequence of coexisting R_0 and R_4 or L_4 layers. Since twin boundaries are visible in the (001) plane, the composition surface must pass through the silicate layers. Figure 5 represents a possible layer geometry for such a twin. Note that the ring symmetry in the immediate vicinity of the composition surface has been represented as the ideal 4*mm*. The ideal layer can act as an efficient interface between any two of the four gillespite II layer orientations.

Since R_0/R_4 and R_0/L_4 twins are observed, one might also expect the coexistence of R_0 and L_0 layers. However, the sequence $(\cdots R_0R_0R_0|L_0L_0L_0\cdots)$ will not result in a distinctive diffraction geometry. Twinning of this type might explain, in part, anomalously high oxygen temperature factors of gillespite II (Hazen and Burnham, 1975).

Gillespite polytypes

The existence of several different layer orientations in gillespite I and II implies the possible occurrence of stacking polytypes. In both polymorphs a completely disordered stacking of layers will yield an average diffraction pattern similar to the ideal $P\,4/n\,2_1/m\,2/m$ structure. Two more-likely polytypes are a tetragonal 8 A $(RRRR\cdots)$ or $(LLLL\cdots)$ form which would have space group $P\,4\,2_1\,2$, and an orthorhombic 16 A $(R_0L_0R_0L_0\cdots)$ polytype with space group $P\,2/n\,2_1/c\,2_1/c$. Further studies on gillespite and its isomorphs (*e.g.*, $CaCuSi_4O_{10}$, $SrCuSi_4O_{10}$, $BaCuSi_4O_{10}$) may reveal the existence of these and other stacking polytypes.

Conclusions

Structures which may be represented as periodically arranged sub-units of high pseudo-symmetry frequently display complex twinning, stacking, and transformation behavior. The pseudo-hexagonal silicate layers of most sheet silicates are well-known in this regard, and the rarer gillespite structure has now been shown to be another example. The pseudo-4*mm* layers of gillespite I and II allow a variety of twinning and polytypism, and provide the key to understanding mechanisms of the gillespite transformation.

Acknowledgments

The author gratefully acknowledges the aid and advice of Dr. M. G. Bown and Professor C. W. Burnham. This research was supported by the NATO Postdoctoral Fellowships in Science program.

References

Hazen, R. M. and C. W. Burnham (1974) The crystal structures of gillespite I and II: A structure determination at high pressure. *Am. Mineral.*, *59*, 1166–1176.

——— and ——— (1975) The crystal structure of gillespite II: correction and addendum. *Am. Mineral.*, *60*, 937–938.

Huggins, F., H. K. Mao and D. Virgo (1976) Gillespite at high pressure: results of a detailed Mössbauer study. *Carnegie Inst. Wash. Year Book*, *75*, 756–758.

Merrill, L. and W. Bassett (1974) Miniature diamond anvil pressure cell for single crystal X-ray diffraction studies. *Rev. Sci. Instrum.*, *45*, 290–294.

Strens, R. G. J. (1966) Pressure-induced spin-pairing in gillespite, $BaFe(II)Si_4O_{10}$. *Chem. Commun.*, *21*, 777–778.

Manuscript received, June 9, 1976; accepted for publication, December 28, 1976.